Published by
NIGERIAN SOCIETY OF PHYSICAL SCIENCES
Available online @ https://journal.nsps.org.ng/index.php/jnsps

J. Nig. Soc. Phys. Sci. 8 (2026) 3322

Journal of the Nigerian Society of Physical Sciences

Adsorption of dithiazolidine compounds on Fe(110) surface and potential for corrosion inhibition: DFT calculations and adsorption locator/Monte Carlo adsorption simulations

Ekemini Ituen[a,b,*], Peace Madu[c], Adewale Olamoyesan[d], Gospel Asuquo[b], Chibueze J. Olelewe[e], Emmanuel E. Etim[f,*]

[a]*Computational Materials Science Group, TETFund Centre of Excellence in Computational Intelligence, University of Uyo, Uyo, Nigeria*
[b]*Shimmer Center, Tianfu Jiangxi Laboratory, Chengdu 641419, China*
[c]*Department of Chemistry, Ambrose Alli University, Ekpoma, Nigeria*
[d]*College of Science and Computing, Wigwe University, Isiokpo, Nigeria*
[e]*Department of Mechanical Engineering, University of Nigeria, Nsukka, Nigeria*
[f]*Department of Biochemistry, Federal University of Technology, Ikot Abasi, Nigeria*

Abstract

Many corrosion inhibitors act through an adsorption mechanism by forming a stable film that protects the surface from an aggressive environment. The adsorption behaviour of two dithiazolidine derivatives, namely, 3,5-diphenyl-imino-1,2,4-dithiazolidine (DPID) and 3-phenyl-imino-5-chlorophenylimino-1,2,4-dithiazolidine (PCID), on the Fe(110) surface was investigated via density functional theory (DFT) calculations and adsorption locator/Monte Carlo adsorption simulations. Quantum study results reveal that PCID exhibits higher HOMO energy, higher tendency to accept electrons, and greater molecular softness than DPID, though with a smaller HOMO–LUMO energy gap (ΔE = 0.10355 Ha). Fukui function and Mulliken charge analyses led to the identification of sulphur atoms as the most active adsorption centres in both inhibitors. Adsorption locator/Monte Carlo adsorption simulations confirm that both compounds are strongly adsorbed on the Fe(110) surface in a parallel orientation. DPID and PCID afforded adsorption energies of −137.419 kcal mol^{-1} and -147.611 kcal mol^{-1}, respectively, whereas the rigid adsorption energy of PCID reached −149.555 kcal mol^{-1}, a demonstration of stronger surface binding. These highly negative adsorption energies suggest predominantly very strong inhibitor-surface interactions, and that both compounds have theoretical potential as corrosion inhibitors for Fe-based surfaces. However, the adsorption strength and predicted inhibition potential of PCID would be greater compared with DPID, which provides theoretical guidance for rational design and prioritization of dithiazolidine-based corrosion inhibitors for future experimental evaluation.

DOI: 10.46481/jnsps.2026.3322

Keywords: Adsorption, Corrosion inhibition, Dithiazolidine, Fe(110) substrate, HOMO–LUMO

Article History:
Received: 22 February 2026
Received in revised form: 03 June 2026
Accepted for publication: 09 June 2026
Available online: 05 August 2026

Communicated by: B. J. Falaye

1. Introduction

Corrosion constitutes one of the key challenges in industries such as oil and gas transportation, marine engineering, chemical processing, and construction. It impacts material durabil-

*Corresponding author Tel. No.: +234-806-976-2033, +234-907-9192231
Email addresses: ekeminiituen@uniuyo.edu.ng (Ekemini Ituen), emmaetim@gmail.com (Emmanuel E. Etim)

ity and safety, especially metallic materials such as steel and other iron-containing alloys. These alloys are widely deployed in the oil and gas industry because they exhibit high mechanical strength and are cost effective, but they are highly vulnerable to corrosive attack when exposed to environments containing acids, alkalis or saline solutions [1]. Corrosion of steel structural materials has enormous economic impact, and in addition to loss of materials, can also cause equipment failure, increased maintenance cost and environmental hazards.

Several strategies have been explored to mitigate corrosion. Among these, the use of corrosion inhibitors (CIs) is more practical and effective [2]. These CIs are chemicals that retard the corrosion rate when incorporated into the corroding medium. They are mostly derived from organic molecules that contain heteroatoms such as sulphur, oxygen, phosphorus and nitrogen, as well as π-electron systems and multiple bonds [3]. When these features are present in the molecule, they promote strong interactions with metal surfaces through their free electron pairs and enable the inhibitor molecule to adsorb and form a protective film that 'blankets' the metal surface from the attack of corrosive species [4].

The fundamental mechanism that underlies corrosion inhibition is adsorption, and it may occur through physisorption or chemisorption, but this depends on what kind of interactions exist between the CI molecule and the alloy/metal surface aimed to protect [5, 6]. Physisorption involves weak electrostatic interactive forces whereas chemisorption involves stronger coordinate bonding which occurs through electron transfer between the inhibitor and the metal surface [5–10]. In some cases, both physisorption and chemisorption may occur simultaneously, and in such cases, the effectiveness or efficiency of the CI depends on the surface coverage, stability and strength of the surface-adsorbed film formed [11, 12].

Corrosion, its inhibition and the adsorption process can be determined quantitatively through experiments such as electrochemical measurements, weight loss analysis, surface characterizations and the use of adsorption isotherms [8, 13–16]. However, the experimental approach requires expensive instrumentation and long testing periods. The selection of efficient materials may follow extensive trial and error screening of various candidate molecules. Also, experiments alone may not provide detailed molecular-level understanding of active adsorption sites, electronic factors and an adsorption mechanism that governs the inhibitor performance.

A computational approach, including molecular modelling, has therefore emerged as a powerful and cost-effective tool for predicting and interpreting corrosion inhibition behaviour [17, 18]. DFT calculations have been commonly deployed to assess electronic properties such as molecular orbital energies, electronegativity, hardness, and local reactivity descriptors [17, 23–25]. These quantum parameters can provide great insight into the ability of inhibitor molecules to donate electrons to vacant metal d-orbitals or accept back-donated charge from the surface [21]. In addition, MD simulation has enabled direct visualization of adsorption configurations and estimation of adsorption and binding energies, which offers realistic representation of possible inhibitor-surface interactions [17, 19].

Recently, computational studies have been used to successfully demonstrate the advantage of combining DFT and adsorption locator/Monte Carlo adsorption simulations in corrosion science. Organic heterocycles, Schiff bases, azoles, and other compounds rich in N and S atoms have been explored as potential CIs [18, 22–25]. Results have shown that adsorption strength is closely related to molecular structure, planarity, heteroatom distribution, and the effects of attached substituents [17–25]. Despite these advances, the corrosion inhibition potential of many molecules, including some dithiazolidine-based compounds have still not been reported, especially in terms of their adsorption behaviour on iron crystal surfaces.

Dithiazolidine derivatives are attractive corrosion inhibitor candidates because they contain multiple sulphur and nitrogen atoms, as well as conjugated π-systems. Their frameworks seem to be planar which may enhance effective and efficient adsorption on steel surfaces. However, researchers have not exhaustively explored how the structural modifications, such as substitution with halogen or alkyl group, can influence the reactivity electronically as well as the adsorption strength. The specific electronic and geometric features of the dithiazolidine ring system, which contains both sulphur and nitrogen (two critical potential adsorption sites) in a constrained five-membered heterocycle, warrant careful investigation to understand their unique binding mechanisms on Fe surfaces. Furthermore, the influence of asymmetric halogen substitution on the adsorption energetics has not been systematically quantified on this scaffold. Insights into theoretical basis for rational design and optimization of dithiazolidine-based CIs can be obtained if these gaps are addressed, thereby guiding future experimental investigations.

In this work, 3,5-diphenyl-imino-1,2,4-dithiazolidine (DPID) and 3-phenyl-imino-5-chlorophenylimino-1,2,4-dithiazolidine (PCID) were selected as model compounds to probe how electronic perturbations, including both symmetric and asymmetric electron donation and electron withdrawing substituents, could modulate the adsorption strength and surface coverage in this kind of molecules. The present study combines global quantum chemical descriptors (frontier orbitals, electronegativity, hardness), local reactivity analysis (Fukui functions), and adsorption locator/Monte Carlo adsorption simulations to provide multiscale mechanistic insight into the relationship between structure and adsorption of dithiazolidines on Fe(110). This work emphasizes theoretical screening and mechanistic investigation, and the predicted adsorption trends are intended to guide the rational design and prioritization of these compounds for future experimental validation. As applicable with most computational predictions, the results may not represent the exact practical inhibition efficiency in industrial media.

The Fe(110) plane was chosen because, among the low-index surfaces of body-centred cubic (BCC) iron, it has the lowest surface energy and is also the most thermodynamically stable crystallographic surface. Consequently, Fe(110) is the most commonly exposed Fe surface and has been used extensively in computational studies to simulate steel corrosion in various media [26, 27]. To achieve the objectives, the molecu-

lar geometries of each of DPID and PCID were optimized, and some quantum calculations were performed to identify the potential active adsorption sites.Adsorption locator/Monte Carlo adsorption simulations were deployed to model the adsorption configurations of both DPID and PCID on the Fe surface. The energies of adsorption, rigid adsorption and deformation were theoretically quantified from simulation outputs. Using this combination of electronic structure analysis (DFT) and surface interaction models (adsorption locator/Monte Carlo adsorption simulations), theoretical evidence of potential active sites and adsorption strength of the compounds are provided. The findings provide molecular-level insights into corrosion inhibition behaviour of the compounds without engaging in trial and error approach associated with experiments.

2. Computational details

2.1. Construction and optimization of DPID and PCID structures

The three-dimensional Atomistic module of BIOVIA Materials Studio 2017 software was used to construct the molecular structures of DPID and PCID. With this, it was possible to generate their initial geometries in 3D space to obtain realistic molecular conformations before the actual analysis of electronic structure [28]. The geometries were fully optimized using the Forcite module with Condensed-phase Optimized Molecular Potentials for Atomistic Simulations Studies (COMPASS) force field until stable equilibrium configurations were reached. The optimized structures were then used for subsequent analyses.

2.2. DFT calculations

The DMol3 module within Materials Studio was used to perform the calculations to elucidate the electronic properties and reactivity descriptors of DPID and PCID. The calculations were performed on isolated inhibitor molecules in their neutral charge states. Geometry optimization and electronic structure calculations were performed using spin-restricted formalism because both DPID and PCID are closed-shell molecules with no unpaired electrons. The self-consistent field (SCF) procedure was converged to the default Dmol3 convergence criteria, and the geometry optimization was continued until the energy, force, and displacement convergence were satisfied.

No implicit solvation model was applied, hence all calculations correspond to conditions in the gas phase. Similarly, no empirical dispersion correction was included. Frequency calculations were not performed because the objective of the study was not a thermochemical analysis but mainly a comparative evaluation of electronic descriptors and adsorption tendencies. The obtained optimized structures correspond to stable stationary geometries and were subsequently used for the adsorption analysis of interest. All calculations were based on DFT and the exchange-correlation effects were treated using the generalized gradient approximation (GGA) with Becke-exchange and Lee-Yang-Parr correlation (BLYP) functional and double numerical (DNP) basis set with polarization functions, with the basis parameter set to 3.5 for both compounds [28].

The major electronic properties associated with corrosion inhibition, namely, frontier molecular orbitals images and their energies, were computed. The results were used to calculate some reactivity descriptors such as the energy gaps (ΔE), ionization energy (IE), electron affinity (EA), electronegativity (χ), global hardness (η), and global softness (σ) using the following relationships [19, 28]:

$$\Delta E = E_{\mathrm{L}} - E_{\mathrm{H}}, \tag{1}$$

$$IE = -E_{\mathrm{H}}, \tag{2}$$

$$EA = -E_{\mathrm{L}}, \tag{3}$$

$$\chi = \frac{1}{2}(IE + EA), \tag{4}$$

$$\eta = \frac{1}{2}(IE - EA), \tag{5}$$

$$\sigma = \frac{1}{\eta}. \tag{6}$$

where E_{L} is the energy of the LUMO and E_{H} is the energy of the HOMO.

2.3. Fukui function and Mulliken charge analyses

Local reactivity analysis was performed using Fukui indices and Mulliken charge analysis to identify the most probable active adsorption sites on the studied molecules. Electrophilic and nucleophilic regions were predicted from the Fukui functions while the distribution of partial charges was predicted from Mulliken atomic charges [14, 19]. A combination of both analyses allowed screening of the heteroatoms and the functional groups responsible for adsorption.

2.4. Adsorption on Fe(110) by adsorption locator/Monte Carlo adsorption simulations

A crystalline BCC Fe bulk structure was constructed first and the geometry was optimized using the COMPASS force field. The optimized bulk was then cleaved along the Fe(110) crystallographic plane, which represents the most stable and commonly used surface for corrosion simulations [26, 27]. The cleaved surface was expanded into a periodic supercell with dimensions of $12.419 \times 12.419 \times 20.400\ \text{Å}^3$. The Fe(110) slab consisted of three layers, and a vacuum layer of 15 Å was introduced along the surface-normal direction to guard against artificial interactions between periodic images. Each inhibitor molecule was positioned initially at approximately 5 Å above the Fe surface to allow free interaction during simulation.

The Fe(110) slab was treated as a rigid substrate during the adsorption simulation whereas the inhibitor molecules were allowed to relax in order to identify favourable orientations. The Adsorption Locator protocol in Materials Studio for identifying energetically favourable adsorption configurations was deployed. The COMPASS force field was used throughout, and atomic charges were assigned using force field parameters available in the Materials Studio implementation.

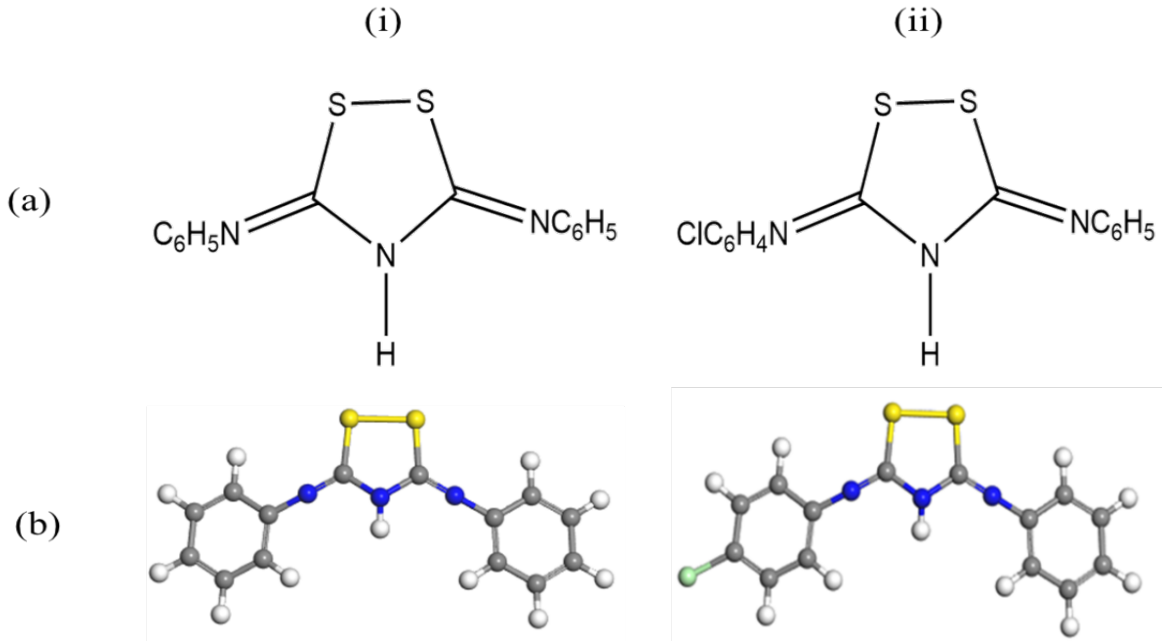

Figure 1: (a) Molecular structures and (b) optimized molecular structures of (i) DPID and (ii) PCID obtained by DFT calculations at the GGA–BLYP/DNP level. [S (yellow); N (blue); C (grey); H (white); Cl (green)].

The adsorption locator tool was applied with the surface region that is defined as the target adsorption zone. The adsorption configurations were then generated from the Materials Studio output as well as the associated energy parameters (in kcal mol^{-1}) such as total energy, adsorption energy, rigid adsorption energy, deformation energy, and differential adsorption energy. The adsorption energy (E_{ads}) was calculated using the relationship

$$E_{ads} = E_{tot} - (E_{sur} + E_{inh}), \tag{7}$$

where E_{tot} is the total energy of the adsorbed inhibitor-Fe(110) system, E_{sur} is the energy of the clean Fe(110) surface, and E_{inh} is the energy of the isolated inhibitor molecule. The rigid adsorption energy E_{rigid}, which represents the interaction strength before structural relaxation of the inhibitor, was calculated from the total energy of the system with the inhibitor kept rigid during adsorption (E_{tot}(rigid)) using the relationship:

$$E_{rigid} = E_{tot(rigid)} - (E_{sur} + E_{inh}). \tag{8}$$

The deformation energy (E_{def}), which is a measure of the structural adjustment of the inhibitor upon adsorption, was evaluated using the relationship:

$$E_{def} = E_{ads} - E_{rigid}. \tag{9}$$

The differential adsorption energy (E_{dif}), was also obtained from the simulation output and is numerically equal to the adsorption energy for a single-molecule adsorption considered in this study. Based on the objectives of the present work, the study employed Monte Carlo-style Adsorption Locator and energy-minimization procedures and not long production molecular dynamics trajectories. As a result, ensemble averaging, equilibration time, and trajectory-based statistical analyses were not performed.

3. Results and discussion

3.1. Geometry optimization

The optimized structures of DPID and PCID are presented in Figure 1 along with their molecular structure. Geometry optimization as the first step in computational adsorption (corrosion inhibition) studies is essential because the conformation of the molecule will influence the adsorption behaviour, surface coverage and mode of inhibitor-surface interaction. Both molecules attained stable minimum energy configurations after full optimization. This indicates that the obtained geometries are energetically favourable structures and are suitable for subsequent quantum chemical and adsorption simulations [28]. The obtained structures afforded largely planar frameworks, with the dithiazolidine ring system and the attached aromatic substituents remaining approximately coplanar.

Planarity is very crucial to corrosion inhibition because flat molecules often align more effectively on the substrate surface, thereby increasing the contact between the inhibitor and the substrate. Theoretically, planar configuration is expected to maximize interaction and promote stronger adsorption, better surface coverage and improved protective layer against corrosive species [29, 30]. The aromatic rings and heteroatoms in the planar system provide multiple adsorption sites for possible coordination with vacant d-orbitals of Fe.

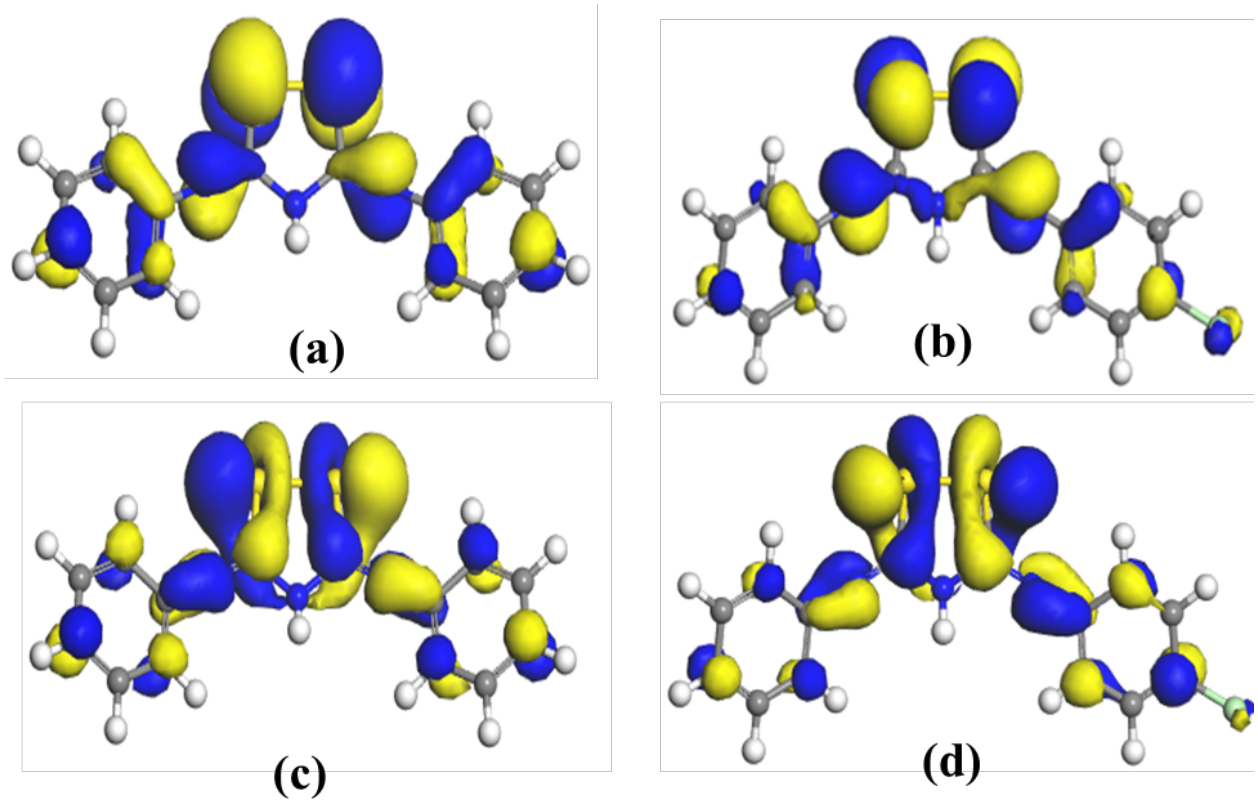

Figure 2: (a) HOMO diagram of DPID; (b) HOMO diagram of PCID; (c) LUMO diagram of DPID; and (d) LUMO diagram of PCID obtained by DFT calculations at the GGA–BLYP/DNP level.

Table 1: Estimated parameters from quantum chemical calculations for DPID and PCID.

Molecule	E_H (Ha)	E_L (Ha)	ΔE (Ha)	IE (Ha)	EA (Ha)	χ (Ha)	η (Ha)	σ (Ha^{-1})
DPID	-0.20490	**-0.04597**	**0.15893**	**0.20490**	0.04597	**0.12543**	**0.07946**	12.58494
PCID	**-0.17691**	-0.07336	0.10355	0.17691	**0.07336**	0.12514	0.05178	**19.31248**

3.2. Molecular orbital energies

Quantum chemical calculations are useful in elucidating molecular reactivity of potential corrosion inhibitor molecules. In Table 1, the obtained parameters are presented with the higher value in bold. The values of E_L, E_H and ΔE indicate the tendency of the molecule to accept electrons, donate electrons and its reactivity tendency towards the metal surface, respectively [3]. Results reveal that PCID has higher E_H and conversely, its E_L, and ΔE are lower than that of DPID. This implies that PCID has higher tendency to donate electrons to and accept electrons from the Fe surface while exhibiting higher reactivity than DPID. The high value of PCID could be attributed to the presence of chlorine substituent.

In corrosion inhibition, the E_H reflects that PCID has a stronger electron-donating capability than DPID. This property favours adsorption through coordinate bonding with the Fe(110) surface. In addition, PCID shows lower HOMO–LUMO energy gap (ΔE= 0.10355 Ha) than DPID (0.15893 Ha). A smaller ΔE is usually associated with higher molecular reactivity and stronger interaction with metal surfaces [3]. Therefore, the lower ΔE value of PCID suggests, as a qualitative indicator only, that it may interact more likely with Fe surface. This implies that PCID may have a relatively higher tendency to interact electronically with the Fe surface compared with DPID and is theoretically predicted to exhibit better corrosion inhibition performance on the Fe surface. However, these observations are qualitative in nature and could be validated only experimentally.

3.3. Other molecular reactivity indices

Other molecular reactivity indices estimated are ionization energy, electron affinity, electronegativity, global hardness, and global softness and the results are presented in Table 1. These indices, in addition to frontier orbital energies, also provide understanding on the adsorption tendency of inhibitor molecules on metal surfaces. The IE reflects how easily a molecule can release electrons for interaction with the metal surface. From results, PCID afforded a lower IE (0.17691 Ha) than DPID (0.20490 Ha) and this indicates that PCID can donate electrons more easily, which supports stronger adsorption on Fe(110) sur-

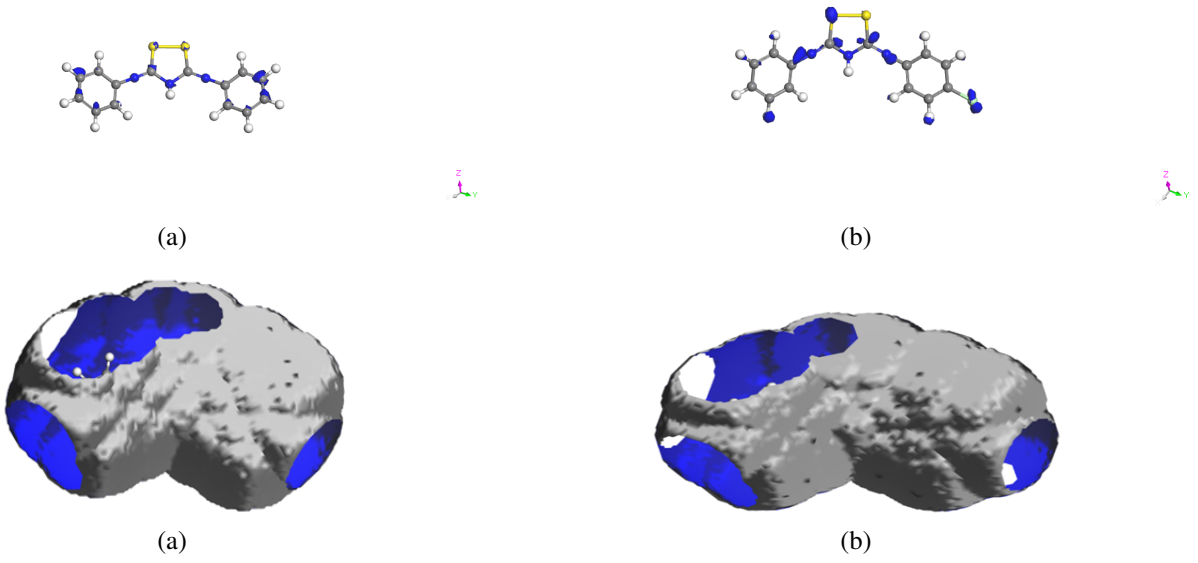

Figure 3: Fukui nucleophilic field (upper panel) and electrophilic field (lower panel) of (a) DPID and (b) PCID obtained by DFT calculations at the GGA–BLYP/DNP level.

face [31]. The *EA* can describe the ability of the molecule to accept electrons. PCID has higher *EA* (0.07336 Ha) than DPID (0.04597), which indicates that PCID would exhibit greater tendency to accept electron density. This portrays that PCID may be more favourably disposed for interactions involving electron back-donation with the Fe surface [32].

The hardness and softness parameters are also essential indicators of molecular reactivity. When a molecule is soft, it reacts more and can form stronger adsorptive interactions with metal/alloy surfaces [16, 32]. From the results, PCID exhibits lower hardness (0.05178 Ha) and higher softness (19.31248 Ha^{-1}) than DPID, which has hardness of 0.07946 Ha and softness of 12.58494 Ha^{-1}. With respect to electronegativity, PCID (0.12514 Ha) and DPID (0.12543) show very close values, and this signifies that their electron-attracting tendencies are comparable. In essence, electronegativity alone does not provide decisive distinction between the two molecules [16, 17]. Generally, the reactivity indices suggest that PCID is electronically softer, with a higher tendency to accept electrons than DPID, while both molecules would exhibit comparable electronegativity. These descriptors support the theoretical prediction that PCID may interact more favourably with Fe(110) surface, although they should be interpreted as qualitative indicators and not as direct measures of corrosion inhibition performance.

3.4. Potential adsorption sites

Understanding of the particular atomic centre(s) that could be responsible for adsorption is essential for explaining the mechanism of action of organic CIs. Therefore, the most probable adsorption site on DPID and PCID were identified using a combination of molecular orbital distribution analysis, Fukui function analysis and Mulliken atomic charge calculations. .

3.4.1. Frontier molecular orbital distribution

In Figure 2, the distributions of HOMO and LUMO orbitals in space are displayed for both molecules. The regions that may take part in electron donation and/or acceptance during adsorption can easily be visualized. The HOMO electron density of both molecules is mainly concentrated around the dithiazolidine ring, and strongly localized on the S atoms and C=N linkage. The aromatic phenyl rings also contribute to HOMO distribution through their π-electron systems although the highest density is observed near the core of the heteroatoms. This implies that the sulphur atoms are the most likely centres for electron donation to the vacant d-orbitals of Fe, which suggests a theoretical tendency towards coordinate-type of interactions during adsorption. In PCID, additional HOMO density is slightly extended toward the substituted phenyl ring, suggesting that the chlorine-containing group may influence the electronic distribution and enhance surface interaction.

On the other hand, the LUMO distribution can be mainly seen over the dithiazolidine ring and parts of the aromatic substituents. Thus, these are the regions that can act as electron-accepting sites to allow possible back-donation of electron density from the Fe surface into the inhibitor molecule. Such donor–acceptor interactions are predicted to strengthen adsorption and may also contribute to improved inhibition efficiency. Therefore, the dithiazolidine core, especially the sulphur atoms, can be considered as the dominant electronic region involved in bonding with the Fe(110) surface.

3.4.2. Analysis of the Fukui function

Based on the Mulliken gross atomic populations, the condensed Fukui functions were calculated by following the finite-difference approach [33]. The calculations were carried out at the optimized geometry of the neutral molecule so as to obtain

Table 2: Fukui indices for nucleophilic and electrophilic attack of DPID and PCID.

DPID		PCID	
f_k^+	f_k^-	f_k^+	f_k^-
S (1) **0.172**	S (1) **0.186**	S (1) **0.171**	S (1) **0.161**
S (2) **0.172**	S (2) **0.186**	S (2) **0.171**	S (2) **0.161**
C (3) 0.025	C (3) -0.012	C (3) 0.012	C (3) -0.004
N (4) 0.011	N (4) 0.011	N (4) 0.013	N (4) 0.008
C (5) 0.025	C (5) -0.011	C (5) 0.030	C (5) -0.004
N (6) **0.038**	N (6) **0.072**	N (6) **0.033**	N (6) **0.087**
N (7) **0.038**	N (7) **0.073**	N (7) **0.039**	N (7) **0.092**
C (8) -0.004	C (8) -0.008	C (8) 0.001	C (8) -0.010
C (9) -0.004	C (9) -0.008	C (9) -0.005	C (9) -0.012
C (10) 0.022	C (10) 0.019	C (10) 0.019	C (10) 0.015
C (11) 0.001	C (11) 0.003	C (11) 0.002	C (11) 0.004
C (12) 0.038	C (12) 0.033	C (12) 0.032	C (12) 0.028
C (13) 0.001	C (13) 0.003	C (13) 0.002	C (13) 0.004
C (14) 0.020	C (14) 0.019	C (14) 0.018	C (14) 0.015
C (15) 0.020	C (15) 0.018	C (15) 0.022	C (15) 0.017
C (16) 0.002	C (16) 0.003	C (16) 0.005	C (16) 0.007
C (17) 0.037	C (17) 0.032	C (17) 0.038	C (17) 0.028
C (18) 0.001	C (18) 0.003	C (18) 0.005	C (18) 0.006
C (19) 0.021	C (19) 0.018	C (19) 0.022	C (19) 0.017
H (20) 0.025	H (20) 0.024	H (20) 0.024	H (20) 0.023
H (21) 0.026	H (21) 0.026	H (21) 0.022	H (21) 0.023
H (22) 0.038	H (22) 0.038	H (22) 0.036	H (22) 0.037
H (23) 0.045	H (23) 0.045	H (23) 0.042	H (23) 0.042
H (24) 0.038	H (24) 0.038	H (24) 0.037	H (24) 0.038
H (25) 0.023	H (25) 0.021	H (25) 0.017	H (25) 0.021
H (26) 0.023	H (26) 0.021	H (26) 0.021	H (26) 0.022
H (27) 0.038	H (27) 0.038	H (27) 0.038	H (27) 0.037
H (28) 0.045	H (28) 0.045	H (28) 0.037	H (28) 0.036
H (29) 0.038	H (29) 0.038	H (29) 0.027	H (29) 0.024
H (30) 0.026	H (30) 0.026	Cl (30) 0.071	Cl (30) 0.075

vertical condensed Fukui indices. For each optimized neutral molecule containing N electrons, single-point calculations were carried out at the same level of theory for the neutral species (N), cationic species $(N-1)$ as well as the anionic species $(N+1)$, where $(N+1)$ and $(N-1)$ correspond to total charges of -1 to $+1$, respectively [33]. The charged species were treated as open-shell doublet systems. For a given atom, k, the Fukui indices were obtained using:

$$f_k^+ = P_k(N-1) - P_k(N), \tag{10}$$

$$f_k^- = P_k(N) - P_k(N+1), \tag{11}$$

where $P_k(N)$, $P_k(N+1)$, and $P_k(N-1)$ are the Mulliken gross atomic populations of atom k in the neutral, cationic, and anionic species, respectively. Equivalently, using Mulliken atomic charges q_k directly, the same quantities may be expressed as

$$f_k^+ = q_k(N) - q_k(N-1), \tag{12}$$

$$f_k^- = q_k(N+1) - q_k(N). \tag{13}$$

Following this convention, f_k^+ is used to identify the atomic site that is most capable of accepting electron density, whereas f_k^- identifies the site from which electron density is most easily removed. Therefore, f_k^+ relates to nucleophilic attack or electron back-donation from the Fe surface to the inhibitor, while f_k^- relates to electrophilic attack or electron donation from the inhibitor molecule to vacant orbitals of Fe atoms.

The N atoms could also contribute to local reactivity, especially N(6) and N(7), although their Fukui indices were lower than those of the sulphur atoms. In PCID, the Cl atom also shows observably large values, and this could signify that the chloro-substitution may influence the electronic distribution of the molecule. Overall, the sulphur atoms remain the dominant potential adsorption centres for both DPID and PCID. Some C atoms, such as C(8) and C(9) in both molecules exhibit small negative Fukui values. The magnitude of these values is very small, hence they may have arisen from charge redistribution associated with the Mulliken population-based finite-difference procedure used [34]. Such values may also result from non-local polarization of the electron density due to electron addition or removal. Instead of implying negative reactivity, they may most likely indicate that the atoms would have negligible contribution to the adsorption process.

3.4.3. Distribution of Mulliken atomic charge

Mulliken population analysis can provide additional insight into identifying the sites that are electron-rich and which can interact strongly with metal atoms [35]. The obtained Mulliken charges for DPID and PCID are listed in Table 3 while the fields are displayed in Figure 3. The S atom can be seen to carry significant negative charge (DPID: -0.142 and -0.140; PCID: -0.170 and -0.170). This indicates that they are centres around which electron density is very high. The negative charge favours efficient adsorption because they can donate electron density to the metal. Nitrogen (N(4)), in addition to S centres, shows the most negative in both molecules. This indicates that N also contributes to adsorption through electron donation although the S atoms may remain the dominant donor sites.

Chlorine substitution in PCID alters charge distribution slightly, which likely induces higher negative charges on the active sulphur centres, and would lead to increased overall adsorption tendency of PCID compared with DPID. On comparing Figure 2 with Fukui indices and Mulliken charges, there is strong correlation that the S atoms in the ring are the most potent adsorption centres in both molecules while the nitrogen atoms also contribute but to lesser extent.

3.5. Adsorption locator/Monte Carlo adsorption simulations

Adsorption locator/Monte Carlo adsorption simulations approach has been reliably deployed to understand and describe adsorption behaviour of CI molecules on surfaces of substrates they are intended to protect under realistic conditions [36]. While quantum chemical descriptors provide information on electronic reactivity, adsorption locator/Monte Carlo adsorption simulations afford direct evidence of adsorption configuration, binding stability and the energetics of inhibitor-surface interactions. These factors are essential because effective corrosion

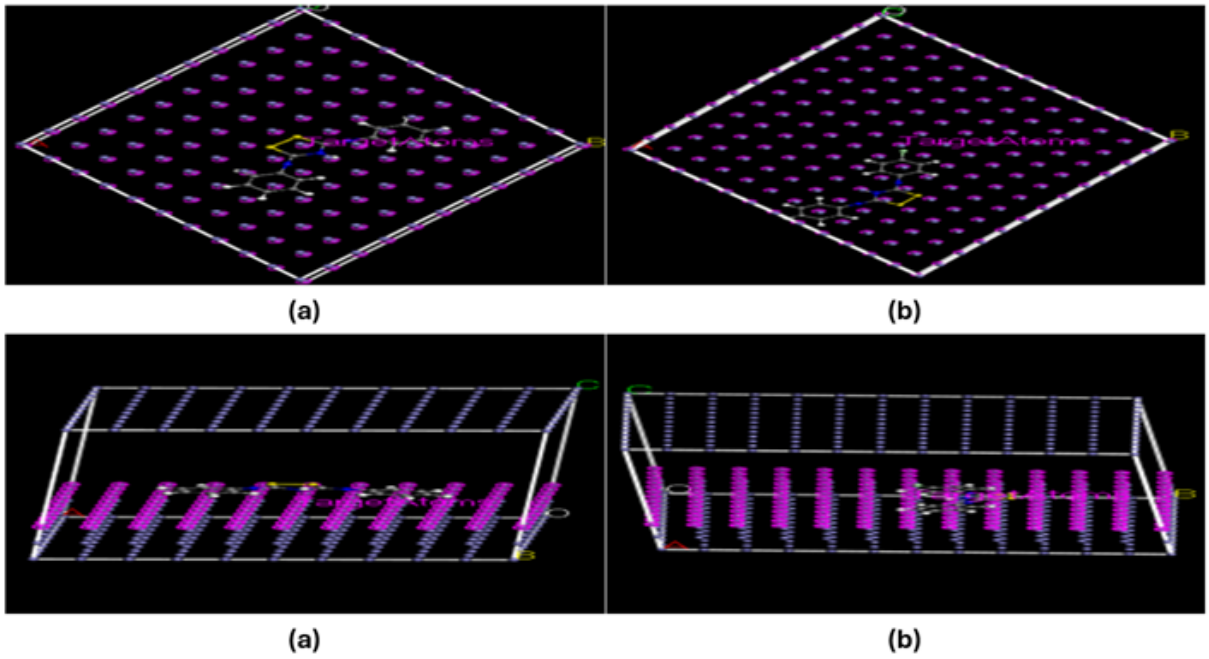

Figure 4: Front (upper panel) and side (lower panel) views of the adsorption arrangement of (a) DPID and (b) PCID on the Fe(110) crystal obtained from adsorption locator/Monte Carlo adsorption simulations using the Forcite module and the COMPASS force field.

inhibitors must adsorb strongly and persistently on the surface to form a protective film that drives the corrosion inhibition in an aggressive environment.

The most stable adsorption configurations of DPID and PCID on the Fe(110) surface are displayed in Figure 4. During adsorption, both molecules assume an almost parallel orientation relative to the iron surface. This configuration favours adsorption because it maximizes surface contact area and allows multiple heteroatoms and π-electron regions to interact simultaneously with surface iron atoms. Because of the extended surface coverage, the molecule readily forms a compact barrier layer which reduces the access of the corrosive species to the surface. This implies strong adsorption and efficient inhibition potential.

The adsorption locator/Monte Carlo adsorption simulations afforded energy parameters that were used to predict adsorption strength and stability, and these parameters are presented in Table 4 in kcal mol^{-1}. The adsorption energy is an indicator of the energy change that accompanies the binding of inhibitor to the surface of the metal, and more negative values correspond to stronger and more stable adsorption. The results reveal that the adsorption energies of DPID and PCID were -137.419 kcal mol^{-1} and -147.611 kcal mol^{-1}, respectively. Since the E_{ads} for PCID is more negative than that of DPID, it can be inferred that PCID is associated with a stronger thermodynamic driving force for adsorption. The magnitude of the difference, approximately 10.2 kcal mol^{-1}, is significant and portrays that PCID would exhibit substantially enhanced surface affinity compared with DPID.

The E_{rigid} values are more negative than the E_{ads} values. This reflects the intrinsic interaction strength between the inhibitor and the Fe surface before the occurrence of molecular relaxation. The relatively small deformation energies indicate that both molecules would undergo minimal structural distortion during adsorption. However, PCID with a lower E_{def}, would require less energetic adjustment to attain its optimal adsorbed geometry. This lower energetic cost of structural adjustment, in addition to its higher adsorption energy, demonstrates that PCID would not only bind more strongly to the surface but would also bind with greater conformational stability. Thus, the energetic characteristics of both molecules point to the possibility that PCID would form more resilient and persistent protective film that resists desorption than DPID under similar corrosion conditions [37]. Inhibitor layers that result from strong adsorptive interactions can be theoretically predicted to be more stable and less susceptible to displacement by corrosive conditions, and can offer long term corrosion protection.

This trend is also supported by the total energy values obtained from the simulations. It can be observed that PCID exhibits lower E_{tot} than DPID suggesting that PCID is energetically more stable than DPID. Combining a more negative adsorption energy, lower deformation energy, and greater overall stability signifies that PCID would form more compact, durable, and persistent protective film on Fe surface, and consequently, better corrosion inhibition. In general, the results of MD simulation demonstrate that both molecules would exhibit strong adsorption on Fe(110) surface with a parallel orientation, with PCID showing a consistently stronger predicted adsorption tendency than DPID across most of the computed descriptors.

Table 3: Mulliken atomic charges of DPID and PCID.

DPID		PCID	
S (1)	-0.142	S (1)	-0.170
S (2)	-0.140	S (2)	-0.170
C (3)	0.399	C (3)	**0.466**
N (4)	**-0.412**	N (4)	**-0.455**
C (5)	**0.402**	C (5)	0.464
N (6)	-0.379	N (6)	-0.418
N (7)	-0.381	N (7)	-0.415
C (8)	0.214	C (8)	0.254
C (9)	0.212	C (9)	0.260
C (10)	-0.103	C (10)	-0.124
C (11)	-0.091	C (11)	-0.095
C (12)	-0.105	C (12)	-0.110
C (13)	-0.088	C (13)	-0.096
C (14)	-0.103	C (14)	-0.120
C (15)	-0.099	C (15)	-0.115
C (16)	-0.090	C (16)	-0.058
C (17)	-0.103	C (17)	-0.009
C (18)	-0.090	C (18)	-0.058
C (19)	-0.104	C (19)	-0.118
H (20)	0.236	H (20)	0.245
H (21)	0.080	H (21)	0.083
H (22)	0.090	H (22)	0.097
H (23)	0.088	H (23)	0.095
H (24)	0.090	H (24)	0.098
H (25)	0.088	H (25)	0.096
H (26)	0.087	H (26)	0.104
H (27)	0.089	H (27)	0.111
H (28)	0.087	H (28)	0.111
H (29)	0.089	H (29)	0.092
H (30)	0.079	Cl (30)	-0.147

Table 4: Adsorption energy and related energies obtained from adsorption locator/Monte Carlo adsorption simulations.

Parameters (kcal mol^{-1})	DPID	PCID
Total energy	-165.657	**-176.822**
Adsorption energy	-137.419	**-147.611**
Rigid adsorption energy	-139.653	**-149.555**
Deformation energy	2.234	1.944
Differential energy of adsorption	-137.419	**-147.611**

4. Conclusion

This study presents results of a computational investigation of the adsorption behaviour of two dithiazolidine compounds, DPID and PCID, on the Fe(110) surface and its implication on corrosion inhibition, using DFT and adsorption locator/Monte Carlo adsorption simulations. Quantum chemical results reveal that the electronic properties of both DPID and PCID favour interaction with Fe. The PCID molecule exhibits higher HOMO energy and lower HOMO–LUMO gap, hence higher reactivity than DPID. From local reactivity analyses using Fukui indices and Mulliken charge distribution, the main active adsorption and electron donor-acceptor interaction sites in both molecules are the sulphur atoms, and to a lesser extent nitrogen centres. Adsorption locator/Monte Carlo adsorption simulations simulations provided evidence of strong adsorption of both molecules on Fe(110) surface through surface coverage of the molecules at parallel orientations. The adsorption energy values were highly negative for both compounds but PCID afforded stronger adsorption strength, greater energetic stability, and lower deformation energy compared with DPID, suggesting its superior potential to theoretically form stable adsorbed barrier layer. The combined DFT and MD findings demonstrate that both PCID and DPID are theoretically promising corrosion inhibitor candidates for Fe surfaces based on their predicted adsorption behaviour, with greater theoretical potential expectations from PCID. Experimental validations using electrochemical and weight loss measurements, as well as surface characterization techniques are recommended to confirm these computational predictions.

Data availability

The datasets analyzed during the study are available from the corresponding author on reasonable request.

Declaration of competing interest

The authors declare that there are no competing interests.

Funding

The authors appreciate the support of the Tertiary Education Trust Fund (TETFund) of the Federal Republic of Nigeria through the TETFund Centre of Excellence in Computational Intelligence Research.

Acknowledgements

The authors appreciate the support of Tertiary Education Trust Fund (TETFund) of Federal Republic of Nigeria, through the TETFund Centre of Excellence in Computational Intelligence Research as well as the Management of the University of Uyo, Uyo, Nigeria.

References

[1] K. Berdimuradov, A. Rasulov, H. Yaxshinorov, J. Abdisattorov, E. Berdimurodov, O. Dagdag & M. Rbaa, *Corrosion in the chemical processing industry*, in *Industrial Corrosion: Fundamentals, Failure, Analysis and Prevention*, S. Zehra, R. Aslam, M. Mobin, & C. Verma. Wiley, (Ed.) Hoboken, USA, 2025, pp. 131–152. https://doi.org/10.1002/9781394301560.ch6.

[2] N. J. Mohammed, M. R. Yusop & N. K. Othman, "Green and nano-based strategies for controlling mild steel corrosion in acidic media: a systematic review", npj Materials Degradation **10** (2026) 16. https://doi.org/10.1038/s41529-025-00726-z.

[3] E. Ituen, L. Yuanhua, C. Verma, A. Alfantazi, O. Akaranta & E. E. Ebenso, "Synthesis and characterization of walnut husk extract-silver nanocomposites for removal of heavy metals from petroleum wastewater and its consequences on pipework steel corrosion", Journal of Molecular Liquids **335** (2021) 116132. https://doi.org/10.1016/j.molliq.2021.116132.

[4] A. Chaouiki, M. Chafiq, Y. G. Ko, A. H. Al-Moubaraki, F. Z. Thari, R. Salghi, K. Karrouchi, K. Bougrin, I. H. Ali & H. Lgaz, "Adsorption mechanism of eco-friendly corrosion inhibitors for exceptional corrosion protection of carbon steel: electrochemical and first-principles DFT evaluations", Metals **12** (2022) 1598. https://doi.org/10.3390/met12101598.

[5] A. Kokalj, "Corrosion inhibitors: physisorbed or chemisorbed?", Corrosion Science **196** (2022) 109939. https://doi.org/10.1016/j.corsci.2021.109939.

[6] A. K. Reddy, Modern Electrochemistry, Plenum Press, New York, USA, 2000. https://www.scribd.com/document/117525559/Modern-Electrochemistry-1-Ionics.

[7] A. Martínez-Mesa & G. Seifert, "Adsorption of molecular hydrogen on nanostructured surfaces", Revista Cubana de Física **31** (2014) 32. https://www.researchgate.net/publication/264550354_Adsorption_of_molecular_hydrogen_on_nanostructured_surfaces.

[8] E. Ituen, O. Akaranta & A. James, "Evaluation of performance of corrosion inhibitors using adsorption isotherm models: an overview", Chemical Science International Journal **18** (2017) 1. https://doi.org/10.9734/CSJI/2017/28976.

[9] S. De Gisi, G. Lofrano, M. Grassi & M. Notarnicola, "Characteristics and adsorption capacities of low-cost sorbents for wastewater treatment: a review", Sustainable Materials and Technologies **9** (2016) 10. https://doi.org/10.1016/j.susmat.2016.06.002.

[10] Y. Artioli, "Adsorption", in Elsevier eBooks, Elsevier, Amsterdam, Netherlands, 2008, pp. 60–65. https://doi.org/10.1016/b978-008045405-4.00252-4.

[11] H. Kumar, V. Yadav, S. K. Saha & N. Kang, "Adsorption and inhibition mechanism of efficient and environment friendly corrosion inhibitor for mild steel: experimental and theoretical study", Journal of Molecular Liquids **338** (2021) 116634. https://doi.org/10.1016/j.molliq.2021.116634.

[12] O. A. Akinbulumo, O. J. Odejobi & E. L. Odekanle, "Thermodynamics and adsorption study of the corrosion inhibition of mild steel by Euphorbia heterophylla L. extract in 1.5 M HCl", Results in Materials **5** (2020) 100074. https://doi.org/10.1016/j.rinma.2020.100074.

[13] N. Setti, A. Barrahi, M. Maatallah, Y. Kaddouri, T. B. Hadda, H. Outada, A. Thakur, R. Touzani, K. Karrouchi, H. A. Abuelizz, B. Dikici, A. Zarrouk & A. Dafali, "Experimental and computational approach on the corrosion inhibition properties of two newly pyrazole derivatives on carbon steel in acid medium", Scientific Reports **15** (2025) 3631. https://doi.org/10.1038/s41598-025-87564-w.

[14] E. Ituen, V. Mkpenie, L. Yuanhua & A. Singh, "Inhibition of erosion corrosion of pipework steel in descaling solution using 5-hydroxytryptamine-based additives: empirical and computational studies", Journal of Molecular Structure **1204** (2020) 127562. https://doi.org/10.1016/j.molstruc.2019.127562.

[15] C. Verma, E. E. Ebenso, L. O. Olasunkanmi, M. A. Quraishi & I. B. Obot, "Adsorption behavior of glucosamine-based pyrimidine-fused heterocycles as green corrosion inhibitors for mild steel: experimental and theoretical studies", The Journal of Physical Chemistry C **120** (2016) 11598. https://doi.org/10.1021/acs.jpcc.6b04429.

[16] H. H. Hammud, W. A. Aljamhi, I. Shawish, N. Hazimah, B. Z. Arfan, M. Haniti, S. A. Hamid, N. S. Sheikh, H. M. Abd El-Lateef, A. Barakat & A. El-Faham, "Experimental and computational anticorrosion behaviors of pyrazole s-triazine/anilino-morpholino derivatives for steel in acidic solutions", ACS Omega **9** (2024) 31714. https://doi.org/10.1021/acsomega.4c02569.

[17] E. Ituen, I. Umana, A. Etuk, S. Shaibu, A. Johnson, V. Mkpenie & U. Inyang, "Computational assessment of structure-activity relationship, adsorption behaviour and significance on corrosion inhibition of some benzothiazole-based compounds", Engineering and Applied Science Letters **8** (2025) 35. https://doi.org/10.30538/psrp-easl2025.0118.

[18] H. Mi, G. Xiao & X. Chen, "Theoretical evaluation of corrosion inhibition performance of three antipyrine compounds", Computational and Theoretical Chemistry **1072** (2015) 7. https://doi.org/10.1016/j.comptc.2015.08.023.

[19] U. Habeeba & N. Raghavendra, "A theoretical approach to the corrosion inhibition of iron (110) in HCl activation by environmental benign four amino acids: MC simulation and DFT studies", Extreme Materials **1** (2025) 1. https://doi.org/10.1016/j.exm.2025.02.001.

[20] Z. El Adnani, M. McHarfi, M. Sfaira, M. Benzakour, A. T. Benjelloun & M. Ebn Touhami, "DFT theoretical study of 7-R-3methylquinoxalin-2(1H)-thiones (R = H; CH3; Cl) as corrosion inhibitors in hydrochloric acid", Corrosion Science **68** (2013) 223. https://doi.org/10.1016/j.corsci.2012.11.020.

[21] S. Elmi, M. M. Foroughi, M. Shahraki, N. Dehdab & M. Shahid, "Computational evaluation of N-thiazolyl-2-cyanoacetamide derivatives on corrosion inhibition of aluminum", Journal of Failure Analysis and Prevention **18** (2018) 887. https://doi.org/10.1007/s11668-018-0476-7.

[22] C. Verma, A. Thakur, R. Ganjoo, S. Sharma, H. Assad, A. Kumar, M. A. Quraishi & A. Alfantazi, "Coordination bonding and corrosion inhibition potential of nitrogen-rich heterocycles: azoles and triazines as specific examples", Coordination Chemistry Reviews **488** (2023) 215177. https://doi.org/10.1016/j.ccr.2023.215177.

[23] N. Lahrache, S. Jebbari, A. Barhoumi, M. Omari, N. Labjar, H. Nasrellah, S. Lakhloufi & S. El Hajjaji, "Synthesis, experimental and theoretical studies on the inhibition of corrosion of C38 steel in a molar hydrochloric acid solution by bis-5,6-methylbenzimidazole-2-thione", Hybrid Advances **11** (2025) 100543. https://doi.org/10.1016/j.hybadv.2025.100543.

[24] N. Betti, A. A. Al-Amiery, W. K. Al-Azzawi & W. N. R. W. Isahak, "Corrosion inhibition properties of Schiff base derivative against mild steel in HCl environment complemented with DFT investigations", Scientific Reports **13** (2023) 8979. https://doi.org/10.1038/s41598-023-36064-w.

[25] M. A. Quraishi, D. S. Chauhan & V. S. Saji, *Heterocyclic Organic Corrosion Inhibitors: Principles and Applications*, Elsevier, Amsterdam, Netherlands, 2020. https://dokumen.pub/heterocyclic-organic-corrosion-inhibitors-principles-and-applications-0128185589-9780128185582.html.

[26] H. H. Rasul, D. M. Mamad, Y. H. Azeez, R. A. Omer & K. A. Omer, "Theoretical investigation on corrosion inhibition efficiency of some amino acid compounds", Computational and Theoretical Chemistry **1225** (2023) 114177. https://doi.org/10.1016/j.comptc.2023.114177.

[27] Z. Chen, Z. Guo & A. A. Fadhil, "Understanding how rebar steel surface anisotropy affects corrosion inhibitor adsorption and performance: from experimental to theoretical studies", Journal of Building Engineering **112** (2025) 113815. https://doi.org/10.1016/j.jobe.2025.113815.

[28] N. I. N. Haris, S. Sobri, Y. A. Yusof & N. K. Kassim, "An overview of molecular dynamic simulation for corrosion inhibition of ferrous metals", Metals **11** (2021) 46. https://doi.org/10.3390/met11010046.

[29] N. Yilmaz, A. Fitoz & K. C. Emregül, "A combined electrochemical and theoretical study into the effect of 2-((thiazole-2-ylimino)methyl)phenol as a corrosion inhibitor for mild steel in a highly acidic environment", Corrosion Science **111** (2016) 110. https://doi.org/10.1016/j.corsci.2016.05.002.

[30] K. Cherrak, O. M. A. Khamaysa, H. Bidi, M. El Massaoudi, I. A. Ali, S. Radi, Y. El Ouadi, F. El-Hajjaji, A. Zarrouk & A. Dafali, "Performance evaluation of newly synthetized bi-pyrazole derivatives as corrosion inhibitors for mild steel in acid environment", Journal of Molecular Structure **1261** (2022) 132925. https://doi.org/10.1016/j.molstruc.2022.132925.

[31] M. Scheffler & C. Stampfl, *Theory of adsorption on metal substrates*, in *Handbook of Surface Science*, Vol. 2, Elsevier, Amsterdam, Netherlands, 2000, pp. 285–356. https://doi.org/10.1016/S1573-4331(00)80009-8.

[32] A. Kokalj, "On the alleged importance of the molecular electron-donating ability and the HOMO–LUMO gap in corrosion inhibition studies", Corrosion Science **180** (2021) 109016. https://doi.org/10.1016/j.corsci.2020.109016.

[33] F. Kayadibi, S. G. Sagdinc & Y. S. Kara, "Density functional theory studies on the corrosion inhibition of benzoin, benzil, benzoin-(4-phenylthiosemicarbazone) and benzil-(4-phenylthiosemicarbazone) of mild steel in hydrochloric acid", Protection of Metals and Physical Chemistry of Surfaces **51** (2015) 143. https://doi.org/10.1134/S2070205115010050.

[34] P. Udhayakala, A. M. Samuel, T. V. Rajendiran & S. Gunasekaran, "DFT study on the adsorption mechanism of some phenyltetrazole substituted compounds as effective corrosion inhibitors for mild steel", Der Pharma Chemica **5** (2013) 111. https://www.researchgate.net/publication/26844

4624.

[35] P. P. Zamora, K. Bieger, A. Cuchillo, A. Tello & J. P. Muena, "Theoretical determination of a reaction intermediate: Fukui function analysis, dual reactivity descriptor and activation energy", Journal of Molecular Structure **1227** (2021) 129369. https://doi.org/10.1016/j.molstruc.2020.129369.

[36] I. B. Obot, N. O. Obi-Egbedi & S. A. Umoren, "Antifungal drugs as corrosion inhibitors for aluminium in 0.1 M HCl", Corrosion Science **51** (2009) 1868. https://doi.org/10.1016/j.corsci.2009.05.017.

[37] A. Kokalj, "Molecular modeling of organic corrosion inhibitors: calculations, pitfalls, and conceptualization of molecule–surface bonding", Corrosion Science **193** (2021) 109650. https://doi.org/10.1016/j.corsci.2021.109650.